# Obstacle Avoidance Algorithm for Unmanned Aerial Vehicle Power Line Detection based on Binocular Vision

SHUHAN YU
Hainan International College,
Communication University of China,
Beijing 100024,
CHINA

*Abstract:* - In recent years, the study of binoculars-based transmission line detection and obstacle avoidance algorithms has gradually gained attention in the development of unmanned aircraft technology. This study aims to study the application of binoculars in transmission line inspections by combining image processing and depth data analysis to improve the navigational and obstacle avoidance capability of unmanned aircraft in complex environments. By constructing efficient visual algorithms, it is possible to identify obstacles in and around power lines in real time, thereby optimizing flight paths and ensuring the smooth progress of detection tasks. In addition, this study will also explore the practical application effects of the algorithm and evaluate its potential value in the field of power inspection.

*Key-Words:* - Drone, Binocular vision, Obstacle avoidance, Line Detection, Electricity, Algorithm.

Received: July 13, 2024. Revised: January 25, 2025. Accepted: April 16, 2025. Published: May 28, 2025.

## 1 Introduction

After a massive investment in electricity grid infrastructure in China, significant achievements have been made in the construction of the country's electricity grid. At present, China has the world's largest electricity grid, and the largest scale substations and transmission in the world, [1]. Very high voltage and very high voltage transmission technologies are also becoming increasingly mature, leading the world. With the continuous improvement of China's power grid achievements, the requirements for inspection efficiency, maintenance intensity, and stable operation of transmission lines will also increase, [2]. However, there are significant differences in environmental conditions in areas where the Chinese power lines are located, and some even have to cross mountains and deep forests. The natural environment is very harsh, and most electrical wiring is installed outdoors, often affected by sharp changes in ambient temperature, the collapse of trees, lightning, and freezing, [3]. Long-term exposure to such environments can easily lead to corrosion, wear and dance, and even serious damage such as tower collapse, bending, and power cord breakage, [4]. If the power plant does not carry out inspections and maintenance on time, even the smallest damage can easily expand, which ultimately leads to significant wiring failures. Therefore, preventing electrical wiring failures and detecting the location of fault points is a very important task in the electrical system. At present, the majority of household electrical line maintenance work is based on regular inspections of employees, [5]. Due to the low efficiency of manual inspections, it is possible that inspections are careless and late. Therefore, power units have begun to study a comprehensive monitoring system that can be installed in transmission lines. The main principle is to use the monitoring system to charge various sensors to monitor the operation of the power grid and to provide timely feedback on problems. While this control system reduces the workload of manual inspections, it also increases the safety and maintenance of the control system, ultimately leading to the failure of this comprehensive control system, [6]. With the development of aircraft technology in China, power units have tried successively to use helicopters, robots, and drones as inspection tools for power lines. Considering costs, technology, and patrol efficiency, drones have advantages over helicopters and robots, [7].

Drones, also known as unmanned aircraft, can be controlled manually or flown independently, [8]. Their main control components are flight control and data acquisition control. Power workers can direct them to fly along transmission lines via land management computers, [9]. At the same time, onboard cameras can record transmission line fault data by photographing, detecting faults in time, and

giving feedback to the ground control computer. Employees can assess whether maintenance is needed on the basis of timely returned fault picture data. As the "eyes" of power line inspection workers, the key technology of drones is intelligent obstacle avoidance route planning during autonomous transmission line inspection, [10].

## 2 Basic Principles of RRT Algorithm

The principle of the Fast Random Path Search (RRT) algorithm is to work in the task area X (including obstacle areas $X_{obs}$ and free areas $X_{free}$). Firstly, set the starting state point $x_{start}$. As the root node of a random tree, it expands a certain distance in each direction of space through random sampling, in the free zone $X_{free}$. Take a random state point $x_{rand}$, as the target point of the root node, traverse the expanded tree nodes of the random tree and select the tree expansion node closest to this state point $x_{nearest}$. As a new growth base point, extend one step towards this state point to obtain a new node in that direction $x_{new}$, [11]. If there is a collision with an obstacle during the expansion process of the step worker, select a new state point and expand it again according to the above rules, [12]. Repeat the above process until a tree expansion node reaches the target state point $x_{goal}$. Until nearby, the final path is backtracked, and the generated backtracking path is the path generated by the RRT algorithm. Figure 1 is a diagram of the node expansion process in the RRT lookup tree.

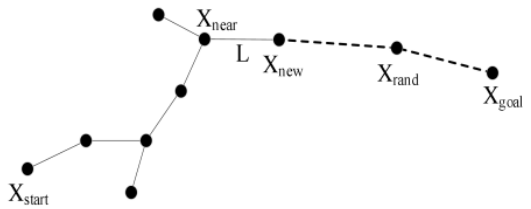


Fig. 1: RRT search tree node expansion process

## 3 Improvement Principle of RRT Algorithm

This article starts with the shortcomings of the RRT algorithm and proposes a segmented P-RRT algorithm. Firstly, change the selection method of the target point. This algorithm takes the i-th power pole as the temporary target point $x_{tgoal(i)}$, and when the search tree successfully expands to $x_{tgoal(i)}$. When using the i-th power pole as a new starting point for expanding the tree $x_{tatart(i)}$, and use the (i+1) th utility pole as the next new temporary target point $x_{tgoal(i+1)}$, repeat this process until it reaches the endpoint $x_{goal}$. The selection of this temporary target point can keep the drone flying within a certain distance range from the power line, in order to obtain a better quality obstacle avoidance trajectory. Then, change the selection method of random state points based on the constraint of the maximum turning angle of the drone and the obstacle zone $X_{obs}$. The distribution of obstacles and the change of random state points $x_{rand}$. The selection rules are used to enhance the purpose orientation of the search tree. Finally, the obtained obstacle avoidance trajectory should fully meet the performance constraints of the drone itself, making the simulation results closer to reality.

### 3.1 Obstacle Collision Detection

The P-RRT algorithm aims to search for an approximate optimal obstacle avoidance trajectory in the task area as quickly as possible, so each time it is $x_{nearest}$ direction $x_{rand}$. Direction extension L is obtained $x_{new}$. When, $x_{nearest}$ give $x_{new}$, the collision detection of the connecting lines (represented by L1 below) needs to be carried out. This problem can be transformed into the principle of line segment intersection in mathematics. If L1 intersects with an edge of a polygon obstacle, it needs to be re selected $x_{rand}$. In order to expand new ones $x_{new}$; If they do not intersect, it indicates that the expansion was successful. The following introduces the detection method for whether the edges of L1 intersect with polygonal obstacles. Firstly, the calculation method and significance of the vector product of two line segments in three-dimensional space will be introduced.

Assuming that the vectors of two line segments in space are $\vec{a}=(x_1,y_1,z_1)$ and $\vec{b}=(x_2,y_2,z_2)$, so its vector product is:

$$\vec{a}\times\vec{b}=\begin{vmatrix}\vec{i} & \vec{j} & \vec{k}\\ x_1 & y_1 & z_1\\ x_2 & y_2 & z_2\end{vmatrix}=(y_1*z_2-z_1*y_2-x_1*z_2,x_1*y_2-y_1*x_2)=-\vec{b}\times\vec{a} \quad (1)$$

According to the right-hand rule of vector product, it can be inferred that if $\vec{a}$ turn at an angle not exceeding 180° $\vec{b}$. If they are counterclockwise, their vector product is greater than 0, and if they are clockwise, it is less than 0. As shown in Figure 2, there are vectors in three-dimensional space $\vec{a}$ and $\vec{b}$. Among them, vectors $\vec{a}$, turn the vector clockwise $\vec{b}$, their vector product is less than 0.

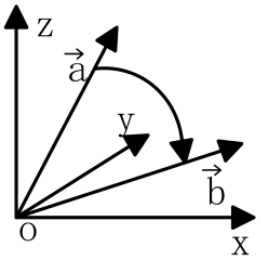

Fig. 2: Three dimensional space vector

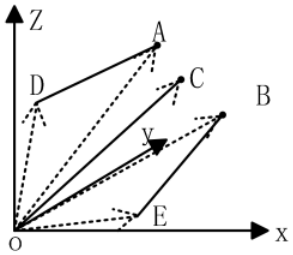

Fig. 3: Schematic diagram of non intersecting spatial vectors

According to this principle, we know that if two points $A(x_1, y_1, z_1)$ and $B(x_2, y_2, z_2)$. In a vector located at the origin $\overrightarrow{OC} = (x_3, y_3, z_3)$, on both sides, then the vectors formed by each of those two points and the origin $\overrightarrow{OA} = (x_1, y_1, z_1)$ and $\overrightarrow{OB} = (x_2, y_2, z_2)$. It will definitely be there $\overrightarrow{OC}$ on both clockwise and counterclockwise sides. That $\overrightarrow{OC} \times \overrightarrow{OA}$ and $\overrightarrow{OC} \times \overrightarrow{OB}$, it must have different numbers, as shown in Figure 3, $\overrightarrow{OC} \times \overrightarrow{OA} > 0, \overrightarrow{OC} \times \overrightarrow{OD} > 0$. Then the vector $\overrightarrow{OA}$ and $\overrightarrow{OD}$, In vector $\overrightarrow{OC}$, on the counterclockwise side of the line, it is impossible for line segment OC and line segment AD to intersect; Similarly, $\overrightarrow{OC} \times \overrightarrow{OB} < 0, \overrightarrow{OC} \times \overrightarrow{OE} < 0$, The line segment BE and the line segment OC cannot intersect.

Therefore, if points A and B are connected to line segment AB, then the vector $\overrightarrow{OC}$. The straight line it is on must intersect with AB. If we consider line segment AB as a vector $\overrightarrow{AB}$, obtain $\overrightarrow{OC} \times \overrightarrow{AB}$. If the conclusion is different, then we can prove that the vector $\overrightarrow{AB}$. The line where it is located intersects with the line segment OC. Since the vector $\overrightarrow{OC}$ intersection of the line and segment AB, vector $\overrightarrow{AB}$. If the line intersects with segment OC, then the two segments must intersect. As shown in Figure 4, where the vector $\overrightarrow{AD}\left(\overrightarrow{BE}\right)$. In vector $\overrightarrow{OC}$, on both sides, it can only be proven that the line segment AD (BE) may intersect with the line segment OC, and it is also necessary to prove the vector $\overrightarrow{OC}$. In vector $\overrightarrow{AD}\left(\overrightarrow{BE}\right)$, on both sides, the vector in the picture is clearly $\overrightarrow{OC}$ be out $\overrightarrow{BE}$. On both sides, the line segment OC and the line segment BE do not intersect; And the vector $\overrightarrow{OC}$ exist $\overrightarrow{AD}$, on both sides, the line segment OC intersects with the line segment AD.

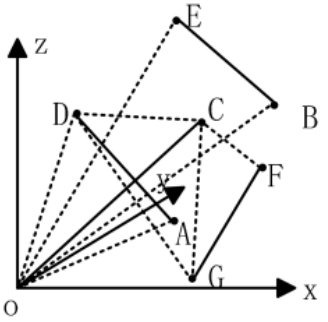

Fig. 4: Schematic diagram of intersection of spatial vectors

Based on the above reduction, the principle of cross-border segments is used to determine whether L1 collides with obstacles in the inspection area, which provides a new method for detecting a drone obstacle collision.

### 3.2 Selection of Random State Nodes

Random status points of traditional RRT algorithms are randomly selected in the search mode without direction of use, [13]. Because RRT algorithms do not expand a new node, they are all related to the selection of random status points. Therefore, if the selection of random status points is not sufficiently optimised, such as the selection of a status point in the obstacle area or deviation from the maximum turning angle limit of the drone, it may ultimately lead to an inadequate overall flight path quality. This article fully takes into account the limitations of the maximum turning angle and obstacle range of the drone $X_{obs}$. Propose random state points under the distribution of obstacles $x_{rand}$. The selection rules.

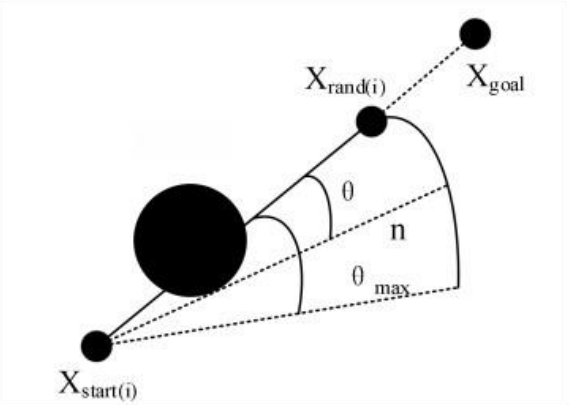

Fig. 5: Constraints on the Selection of Random State Nodes

As shown in Figure 5, according to obstacle collision detection, a temporary new starting point can be determined $x_{tstart(i)}$. Towards the finish line $x_{goal}$, if obstacles are encountered during expansion, random state points need to be re selected $x_{rand}$, support $x_{rand(i)}$ give $x_{tstart(i)}$. The connection is defined as a vector $\overrightarrow{x_{tstart(i)}x_{rand(i)}}$, Passing point $x_{tstart(i)}$. The tangent to the vertex of the obstacle is defined as a vector $\vec{n}$, $\overrightarrow{x_{tstart(i)}x_{rand(i)}}$ and $\vec{n}$. The angle is defined as $\theta$. The maximum turning angle of the drone is $\theta_{\max}$. Random state points that need to be reselected $x_{rand}$. The selection rule is as follows: (1) When $\theta < \theta_{\max}$, When $x_{rand}$, the selection is based on $\theta(\theta_{\max} - \theta)$. As the central angle, $\left|\overrightarrow{x_{tstart(i)}x_{rand(i)}}\right|$ within a fan-shaped area of radius.

(2) When $\theta = \theta_{\max}$, $x_{rand}$, only in vectors $\vec{n}$ Select from above.

(3)When $\theta > \theta_{\max}$, $x_{rand}$, randomly select in the search space.

### 3.3 Improving Algorithm Process

(1) Set starting point $x_{start}$, and endpoint $x_{goal}$. Coordinates, with an extension step length of L, set the starting point $x_{start}$. As a base point for expanding the search tree $x_{tstart(0)}$, Stored in node set E, endpoint $x_{goal}$. As the target point for the extended tree, each power pole serves as a temporary target point for the extended tree $x_{tgoal(i)}$, Among them, i=1,2, n, Where n is the number of utility poles in the simulated terrain;

(2) Position of the first utility pole $x_{tstart(1)}$. As the first temporary target point, randomly select the state point according to the selection rule $x_{rand}$. Then traverse the expanded tree nodes of the random tree and select the distance $x_{rand}$. Recent tree expansion nodes $x_{nearest}$. As a new growth base point (to connect nodes $x_{nearest}$, stored in node set E) direction $x_{rand}$. Expand the direction by one step to obtain a new node in that direction $x_{new}$, give $x_{new}$. The calculation formula is as follows:

$$x_{new} = x_{nearse} + L \times \frac{x_{rand} - x_{nearst}}{\left\| x_{rand} - x_{nearst} \right\|} \quad (2)$$

(3) Connect $x_{new}$ and $x_{nearest}$, use the obstacle collision detection rules to determine if the connection has crossed the obstacle. If not, it indicates that the connection has crossed the barrier. Enlargement has failed and the process must return to phase 2. If so, it means that the connection did not cross the barriers, the expansion was successful, and the node was removed $x_{new}$ Store in node set E and continue with step (4).

(4) $x_{new}$ as a new starting point, continue to expand towards the temporary target point $\left\| x_{tgoal(i-1)} - x_{new} \right\| <= L$. At this point, it indicates that the search tree node has been extended to the (i-1) th power pole, and the (i-1) th power pole is taken as the new starting point for the extended tree $x_{tatart(i-1)}$, And use the i-th power pole as the next new temporary target point $x_{tgoal(i)}$ expand.

(5) When the search tree has expanded to the last temporary target point, i.e. i>n, repeat steps (2) and (3) until $\left\| x_{tgoal(i-1)} - x_{new} \right\| <= L$. At this time, it indicates that the expansion is complete and the endpoint x has been reached.

6) Generate an obstacle avoidance trajectory by connecting two points from each other using node information collected from node set E.

## 4 Comparison and Analysis of Experimental Simulation Results

In order to verify the effectiveness of the P-RRT algorithm proposed in this article, the RRT algorithm, the RRT* algorithm, and the P-RRT algorithm were used to design the trajectory, where L was set to 8. For each algorithm, the time, total number of nodes, number of nodes, effective percentage of nodes (number of nodes) / (total number of nodes) and the importance of transmission lines were compared to complete the design. The experiment was conducted on MATLAB 2018a ThinkPad Intel (R) Core (TM) i3-5005 at 2.00 GHz. The design results of each algorithm are shown in Figure 6.

From Table 1, we can clearly see that under the same simulation environment for overhead lines, the P-RRT algorithm proposed in this paper has shorter search time and higher node effective percentage compared to RRT and RRT * algorithms, reflecting the lower complexity and higher efficiency of the improved P-RRT algorithm; From Figure 6, it can be seen that the trajectory planned by the P-RRT algorithm is more closely related to the power line and more in line with the requirements of unmanned aerial vehicle patrol in practice. Overall, we can conclude that the improved algorithm proposed in this article is effective.

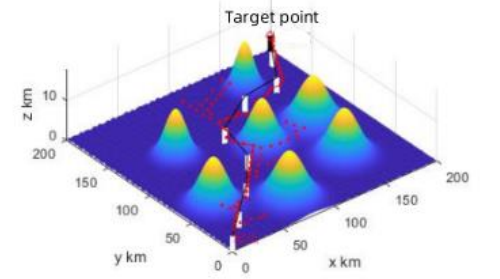


a) RRT algorithm path planning results

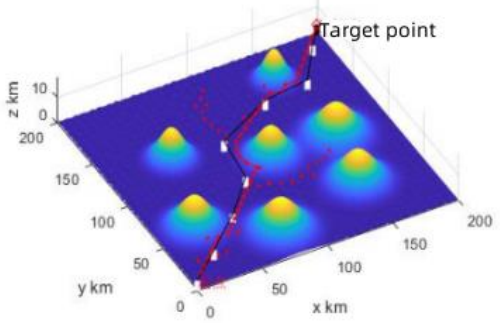


b) RRT * algorithm path planning results

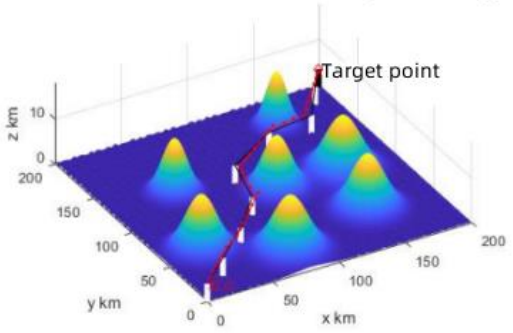


c) P-RRT algorithm path planning results

Fig. 6: Simulation results of algorithm planning for each algorithm

Table 1. Comparison of 10 average values for each algorithm

| Algorithm | Planning time/s | Total number of nodes | Number of trajectory nodes | Effective percentage of nodes/% |
|---|---|---|---|---|
| RRT | 1.4363 | 102 | 36 | 35.30 |
| RRT* | 0.8632 | 86 | 37 | 43.02 |
| P-RRT | 0.7352 | 39 | 30 | 76.92 |

## 5 Conclusion

The research on binocular vision-based unmanned aerial vehicle power line detection and obstacle avoidance algorithm aims to improve the efficiency and safety of unmanned aerial vehicle power line inspection in complex environments. By introducing binocular vision technology, the system can accurately obtain three-dimensional spatial information of power lines, thereby achieving real-time recognition and positioning of the lines and surrounding obstacles. This study not only optimized the flight path planning of drones and reduced collision risks, but also provided reliable technical support for the automation of power inspection tasks. In summary, obstacle avoidance algorithms based on binocular vision have shown promising application prospects in unmanned aerial vehicle power line detection, and have important theoretical significance and practical value.

*References:*

[1] Grant S. Gaze-grasp coordination in obstacle avoidance: differences between binocular and monocular viewing. *Exp. Brain Res.*, 2015, 233(12):3489-505. https://doi.org/10.1007/s00221-015-4421-7.

[2] Zhao J, Allison RS. The role of binocular vision in avoiding virtual obstacles while walking. *IEEE Trans Vis Comput Graph.* 2021, 27(7):3277-3288. https://doi.org/10.1109/TVCG.2020.2969181.

[3] Vejarano F, Alió J, Iribarren R, Lançaan C. Non-miotic improvement in binocular near vision with a topical compound formula for presbyopia correction. *Ophthalmology and Therapy,* 2023, 12:1013-1024. https://doi.org/10.1007/s40123-023-00648-6.

[4] Sharma P, Singh PK, Gautam K, Ganesh S. Role of binocular vision therapy in strabismic and nonstrabismic conditions. *Delhi Journal of Ophthalmology,* 2024, 34(3):166-171. https://doi.org/10.4103/DLJO.DLJO_36_24.

[5] Matsuura A, Sai N, Yamaoka A, Karita T, Mori F. Obstacle avoidance movement-related motor cortical activity with cognitive task. *Exp Brain Res.* 2022, 240(2):421-428. https://doi.org/10.1007/s00221-021-06268-5.

[6] Hossain MM, Iftekhar QS, Naznin SM, Rashid Chowdhury STM, Hasan MM. Binocular vision anomalies in children and young adults and effectiveness of vision therapy. *Delhi Journal of Ophthalmology,* 2023, 32(5):20-25. https://doi.org/10.4103/dljo.dljo_35_23.

[7] Chaturvedi I, Jamil R, Sharma P. Binocular vision therapy for the treatment of Amblyopia--A review. *Indian Journal of Ophthalmology,* 2023, 71(5):1797-1803. https://doi.org/10.4103/IJO.IJO_3098_22.

[8] De Marinis A, Iavernaro F, Mazzia F. A minimum-time obstacle-avoidance path planning algorithm for unmanned aerial vehicles. *Numerical Algorithms,* 2022, 89(4):1639-1661.

https://doi.org/10.1007/s11075-021-01167-w.

[9] Zwierko T, Redondo, Beatríz, Jedziniak W, Molina R, Jiménez R, Vera J. Gaze behaviour during multiple object tracking is dependent on binocular vision integrity. *Ophthalmic & Physiological Optics,* 2024, 44(1):23-31. https://doi.org/10.1111/opo.13225.

[10] Read JCA. Binocular vision and stereopsis across the animal kingdom. *Annu Rev Vis Sci.* 2021, 7:389-415 https://doi.org/10.1146/annurev-vision-093019-113212.

[11] Ma WP, Li WX, Cao PX. Binocular vision object positioning method for robots based on coarse-fine stereo matching. *International Journal of Automation and Computing: English,* 2020, 17(4):562-571. https://doi.org/10.1007/s11633-020-1226-3.

[12] Rawikara SS, Sasongko RA. Dynamic obstacle avoidance system for the unmanned aerial vehicle (UAV). *IOP Conference Series: Materials Science and Engineering,* 2021, 1173(1):12054-12059. https://doi.org/10.1088/1757-899X/1173/1/012054.

[13] Sonny A, Yeduri SR, Cenkeramaddi LR. Q-learning-based unmanned aerial vehicle path planning with dynamic obstacle avoidance. *Applied Soft Computing,* 2023(147):78-82. https://doi.org/10.1016/j.asoc.2023.110773.

**Contribution of Individual Authors to the Creation of a Scientific Article**

The authors equally contributed in the present research, at all stages from the formulation of the problem to the final findings and solution.

**Sources of Funding for Research Presented in a Scientific Article or Scientific Article Itself**

No funding was received for conducting this study.

**Conflict of Interest**

The authors have no conflicts of interest to declare.